NUMERICAL PROBLEMS RELATED TO STEEP MOUNTAINS IN SIGMA-COORDINATES

Z.I. Janjić

Federal Hydrometeorological Institute, Belgrade, Yugoslavia

1. Introduction

An important decision made in the process of designing a numerical model is the choice of vertical coordinate. There exists a variety of possibilities (e.g. Kasahara 1974, 1977). However, each of them is associated with its own problems of representing topography. By far the most frequent choice is the so-called sigma system (Phillips 1957) with coordinate surfaces following the ground surface. A number of other "transformed vertical coordinates" can be constructed in a straightforward manner following the Phillips' idea. The problems which will be discussed here are common for all transformed coordinate systems. Thus, it will suffice to consider only one of them. We shall concentrate on the sigma system, their most popular specimen.

A number of studies dealing with the problem of calculating the pressure gradient force in the sigma system and the related problems has been made (e.g. Arakawa 1972; Arakawa and Lamb 1977; Brown 1974; Corby et al. 1972; Corby et al. 1977; Gary 1973; Gilchrist 1975; Janjić 1977; Kurihara 1968; Phillips 1974; Rousseau and Pham 1971; Smagorinsky et al. 1967; Sundqvist 1975; Tokioka 1978). This paper is devoted to these problems as well. We shall treat them following the ideas of the paper by Janjić (1977). Namely, we shall start our analysis with a discussion of the physical meaning of the pressure gradient force in the sigma system. Some of the problems related to the vertical distribution of variables in numerical models will be discussed as well. A study of the origin of the pressure gradient force error in the sigma system will follow. A rather general method for minimization of the error based on the results of this study will be presented. Also,

a problem related to false vertical staggering of the pressure gradient and Coriolis force will be pointed out. Finally, a systematic derivation of the scheme for the omega-alpha term of the thermodynamic equation ensuring consistency in transformation between the kinetic and potential energy will be presented.

2. General form of the pressure gradient fo force in the sigma coordinate system

The pressure gradient force in the sigma coordinate system may be interpreted as the result of applying the $-\nabla$ operator to the geopotential at a constant pressure level calculated by extrapolation from a neighbouring sigma surface using the hydrostatic equation. Namely, let the geopotential be a function of the form

$$\varphi = \phi(x, y, \zeta) \tag{1}$$

where

$$\zeta = \zeta(p) \tag{2}$$

is a continuous, monotonous function of pressure. Let the pressure gradient force be calculated at a pressure level p^*, and let the corresponding value of ζ be denoted by

$$\zeta^* = \zeta(p) \ . \tag{3}$$

This situation is schematically shown in Figure 1. Using the notation introduced in the figure,

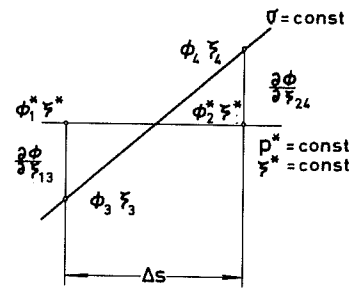

Figure 1. Stencil and notation used to derive the general formula for pressure gradient force in the sigma system.

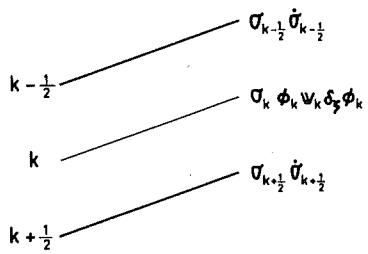

Figure 2. The usual vertical distribution of dependent variables in the sigma system.

at the points 1 and 2 we may write

$$\Phi_1^* = \Phi_3 + \frac{\partial \Phi}{\partial \xi_{13}} (\xi^* - \xi_3) \qquad (4)$$

$$\Phi_2^* = \Phi_4 + \frac{\partial \Phi}{\partial \xi_{24}} (\xi^* - \xi_4) \ . \qquad (5)$$

Here

$$\Phi^* = \Phi(x, y, \xi^*) \ . \qquad (6)$$

Combining the equations (4) and (5) we may write

$$-\frac{\Phi_2^* - \Phi_1^*}{\Delta s} = -\frac{\Phi_4 - \Phi_3}{\Delta s} + \frac{1}{2}\left(\frac{\partial \Phi}{\partial \xi_{13}} + \frac{\partial \Phi}{\partial \xi}\right)\frac{\xi_4 - \xi_3}{\Delta s} - \frac{\frac{\partial \Phi}{\partial \xi_{24}} - \frac{\partial \Phi}{\partial \xi_{13}}}{\Delta s}\frac{1}{2}(2\xi^* - \xi_3 - \xi_4). \qquad (7)$$

Here Δs is the distance between the two points at which the geopotential is being calculated. If Δs is oriented in the direction of the largest variation of geopotential Φ^* along the pressure level p^*, in the limit as Δs tends to zero, the expression (7) tends to

$$-\nabla_p \Phi = -\nabla_\sigma \Phi + \frac{\partial \Phi}{\partial \xi} \nabla_\sigma \xi \ . \qquad (8)$$

As usual, the subscripts p and σ indicate that the ∇ operator is applied along constant pressure and constant sigma surfaces, respectively.

The formula (8) represents the general form of the pressure gradient force in the sigma system in the sense that any of the commonly used expressions can be derived from it by a particular choice of the function ξ. For instance, if we choose

$$\xi = \ln p \ , \qquad (9)$$

the formula (8) takes the form

$$-\nabla_p \Phi = -\nabla_\sigma \Phi - RT \nabla_\sigma \ln p . \qquad (10)$$

3. Discretization of the pressure gradient force, hydrostatic consistency and distribution of variables over grid points in the vertical

Let us for a moment consider the usual vertical distribution of variables over grid points shown schematically in Figure 2. The symbol $\delta_\zeta \Phi$ denotes the simplest finite difference approximation to the derivative of geopotential with respect to ζ, while the other symbols used in the figure have their usual meaning. If we restrict ourselves to, say, x-component of the pressure gradient force, using the notation introduced in Figure 3, similarily as before, we may write

$$-\delta_x \Phi^* \equiv -\frac{\Phi_2^* - \Phi_1^*}{\Delta x} = -\frac{\Phi_4^K - \Phi_3^K}{\Delta x} + \frac{1}{2}(\delta_\zeta \Phi_3^K + \delta_\zeta \Phi_4^K)\frac{\zeta_4^K - \zeta_3^K}{\Delta x} . \qquad (11)$$

The superscripts here indicate the sigma level at which the variables are located. Comparing formulae (7) and (11) it is readily seen that (11) may be interpreted as a result of applying the operator $-\delta_x$ to the values of geopotential obtained by extrapolation via the hydrostatic equation from the level σ_K to the constant pressure level p^* corresponding to $\zeta^* = \frac{1}{2}(\zeta_3^K + \zeta_4^K)$.

However, this extrapolation is sometimes performed in a hydrostatically inconsistent way (Rousseau and Pham 1971; Janjić 1977). Namely, the geopotential at the level σ_K is normally calculated starting from the lowest sigma level at which Φ and $\delta_\zeta \Phi$

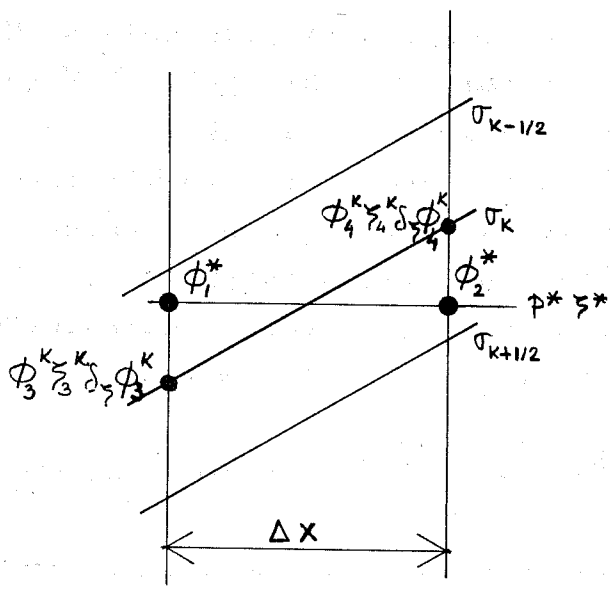

Figure 3. Stencil and notation used to calculate pressure gradient force approximation in case of the usual distribution of variables over grid points in the sigma system.

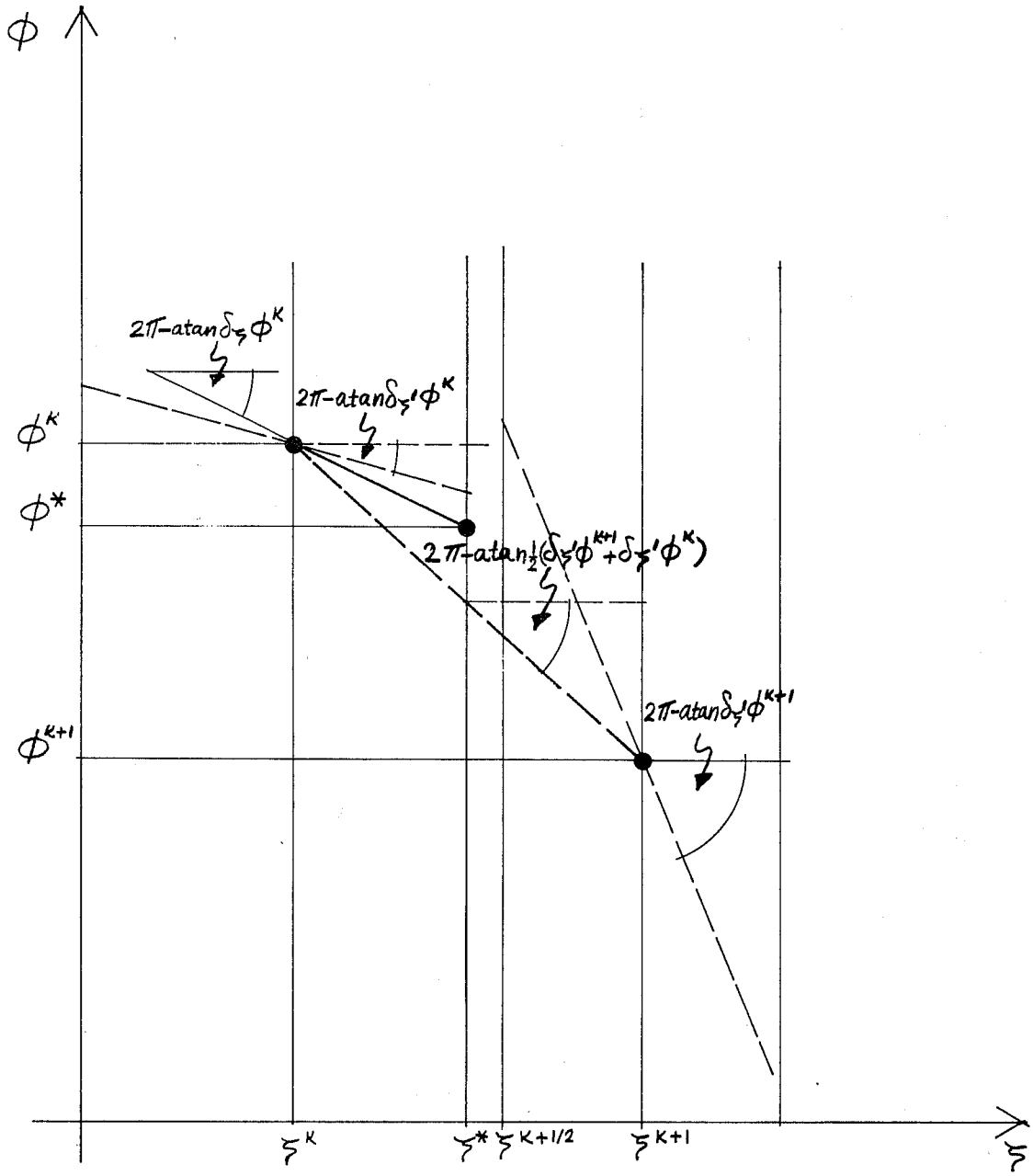

Figure 4. A schematic representation of hydrostatic inconsistency in evaluation of geopotential at a constant pressure level in case of the non-staggered vertical distribution of variables over grid points in the sigma system.

are defined, and adding the thicknesses of the layers above evaluated using a formula of the form

$$\phi^{K+1}-\phi^{K}=\frac{1}{2}(\delta_{\sigma'}\phi^{K+1}+\delta_{\sigma'}\phi^{K})(\sigma'^{K+1}-\sigma'^{K}) \quad . \qquad (12)$$

The function σ' may not necessarily coincide with the function σ (e.g. Arakawa 1972; Arakawa and Mintz 1974/. Of course, the geopotential at the lowest sigma level requires somewhat different treatment, but we shall not consider this problem here. On the other hand, we have used $\delta_{\sigma}\phi^{K}$ to calculate the geopotential ϕ^{*} at the level σ^{*}. This situation is schematically shown in Figure 4. As it can be readily seen, this procedure may be hydrostatically inconsistent in the sense that the geopotential at the sigma levels and at the pressure levels is not calculated integrating the same approximation to the hydrostatic equation. Namely, the formula (12) implies the linear profile of geopotential in between the levels σ^{K+1} and σ^{K}. This profile is represented in the figure by the dashed line connecting the points $(\sigma^{K+1}, \phi^{K+1})$ and (σ^{K}, ϕ^{K}). The slope of this line is defined by $\frac{1}{2}(\delta_{\sigma'}\phi^{K+1} + \delta_{\sigma'}\phi^{K})$ as indicated in the figure. On the other hand, when integrating the hydrostatic equation in between the levels σ^{*} and σ^{K+1}, we are assuming a different linear geopotential profile indicated in the figure by the solid line connecting the points (σ^{*}, ϕ^{*}) and (σ^{K}, ϕ^{K}). This time the slope is defined by $\delta_{\sigma}\phi^{K}$. It should be noted that this inconsistency may occur even if $\sigma=\sigma'$. Namely, as it can be seen from Figure 4, the point (σ^{*}, ϕ^{*}) would again lie off the line connecting the points $(\sigma^{K+1}, \phi^{K+1})$ and (σ^{K}, ϕ^{K}).

An alternative to the distribution of variables shown in Figure 2 is the "staggered" distribution shown in Figure 5. Here we do not specify sigma and σ

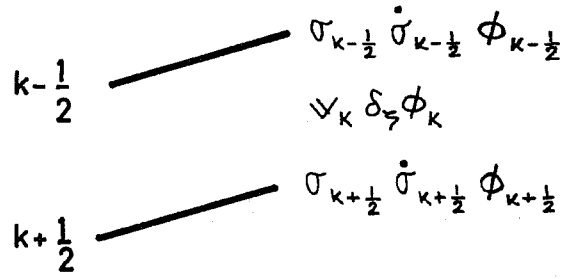

Figure 5. Staggered vertical distribution of dependent variables over grid points in the sigma system.

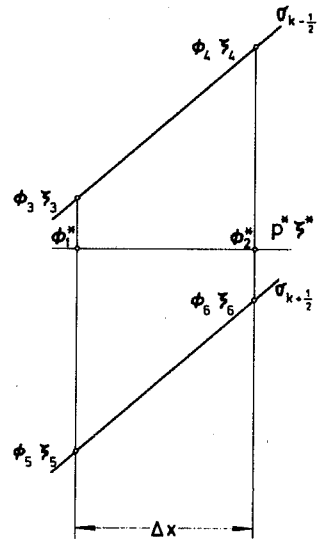

Figure 6. Stencil used to calculate pressure gradient force approximation in case of staggered distribution of variables over grid points in the sigma system.

within the layers. They are defined at the interfaces of the layers only. In this case, the problem of calculating the pressure gradient force in the sigma system reduces to linear interpolation of geopotential to a pressure level p^* corresponding to $\zeta^* = \zeta(p^*)$. Namely, using the notation introduced in Figure 6, in case of a hydrostatically consistent linear interpolation with respect to ζ, we may write

$$-\delta_x \phi^* = -\frac{1}{\Delta x}\left[\phi_4 + \frac{\phi_6 - \phi_4}{\zeta_6 - \zeta_4}(\zeta^* - \zeta_4) - \phi_3 - \frac{\phi_5 - \phi_3}{\zeta_5 - \zeta_3}(\zeta^* - \zeta_3)\right] . \quad (13)$$

It should be noted that the expressions for ϕ^* in (13) can be written in the form

$$\phi_{k-1/2} - \frac{\phi_{k+1/2} - \phi_{k-1/2}}{\zeta_{k+1/2} - \zeta_{k-1/2}}(\zeta^* - \zeta_{k-1/2}) \equiv \overline{\phi}^{\sigma} + \delta_\zeta \phi (\zeta^* - \overline{\zeta}^{\sigma}), \quad (14)$$

where

$$\overline{\phi}^{\sigma} = \tfrac{1}{2}(\phi_{k+1/2} + \phi_{k-1/2}), \quad \overline{\zeta}^{\sigma} = \tfrac{1}{2}(\zeta_{k+1/2} + \zeta_{k-1/2}), \quad \delta_\zeta \phi = \frac{\phi_{k+1/2} - \phi_{k-1/2}}{\zeta_{k+1/2} - \zeta_{k-1/2}} \quad . (15)$$

Using the identity (14) and the notation just introduced, instead of (13) we may write

$$-\delta_x \phi^* = -\delta_x \overline{\phi}^{\sigma} - \overline{\delta_\zeta \phi}^{x} \delta_x (\zeta^* - \overline{\zeta}^{\sigma}) - \overline{(\zeta^* - \overline{\zeta}^{\sigma})}^{x} \delta_x (\delta_\zeta \phi) , \quad (16)$$

where for example,

$$\overline{\delta_\zeta \phi}^{x} = \frac{1}{2}\left(\frac{\phi_6 - \phi_4}{\zeta_6 - \zeta_4} + \frac{\phi_5 - \phi_3}{\zeta_5 - \zeta_3}\right) . \quad (17)$$

If we define the height at which the pressure gradient force is calculated by

$$\zeta^* = \overline{\overline{\zeta}^{\sigma}}^{x} \quad (18)$$

the last term on the right hand side of (16) vanishes. Thus, at this level, the x-component of the pressure

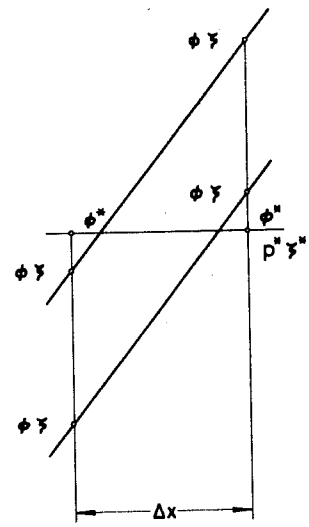

● Figure 7

Figure 7. An example of inconsistency in evaluation of pressure gradient force in case of staggered vertical distribution of variables over grid points in the sigma system.

gradient force approximation takes the form

$$-\delta_x \phi^* = -\delta_x \overline{\phi}^{\sigma} + \overline{\delta_\varsigma \phi}^{x} \delta_x \overline{\varsigma}^{\sigma} \quad . \tag{19}$$

The formula (19) has been derived in a hydrostatically consistent manner. However, it should be noted that in case of very steep slopes of the sigma surfaces and inadequate horizontal resolution, the geopotential at the pressure level defined by (18) may still be calculated inconsistently. This situation is shown schematically in Figure 7.

From a rather general point of view, the preservation of the hydrostatic consistency in the discretized equations seems to be desirable. Namely, it implies a coherent definition of a unique continuous profile of geopotential which, as we have seen, is needed to calculate the pressure gradient force in the sigma system. The requirement for the hydrostatic consistency, as we have defined it here, is obviously equivalent to the assumption that the geopotential vary linearily with ς in between the grid points at which it is calculated integrating the hydrostatic equation. On the other hand, it is rather difficult to make a general assessment as to how the hydrostatic inconsistency affects the accuracy of the pressure gradient force approximation. Some numerical results reported by Phillips (1974) indicate that, at least if $\varsigma \neq \varsigma'$, its influence may be large. For this reason it seems desirable to try to avoid it. The staggered distribution of variables is more suitable for this purpose, since it offers a possibility of calculating the pressure gradient force in a hydrostatically consistent way without any additional effort.

The heuristic arguments discussed so far appear to be much too vague to form a sound basis for judgement as to which of the two distributions should be preferred. A more detailed analysis of the problem has been performed by Tokioka (1978). Namely, starting from a simple idealized situation, he examined the effect of several distributions of the variables over grid points upon simulation of wave propagation in the vertical. It appears that with the both distributions considered here the internal waves are treated as internal, though there is an unavoidable error in the finite difference vertical wavelength. The vertical energy transport is accelerated in the both cases. However, in contrast to the staggered distribution, the non-staggered one allows a computational mode in the vertical. Thus, it appears that the ataggered distribution should be considered as a better choice. For this reason, in the rest of this paper we shall mainly concentrate our attention on this type of grid. However, most of the considerations will be valid for the non-staggered grid as well.

4. Pressure gradient force error in the sigma system and its minimization

To analyze the origin of the additional error of the pressure gradient force in the sigma system as compared to that which occurs, e.g., in the pressure system, consider the situation shown schematically in Figure 8. The two piece-wise linear curves represent geopotential profiles at two adjacent grid points. The heavy dots correspond to the values of geopotential at the interfaces of the sigma layers. As before, the values ϕ_1^* and ϕ_2^*, denoted by crosses, are used to calculate the pressure gradient force at the pressure level corresponding to σ^*. This situation obviously

corresponds to the staggered distribution of variables in the vertical.

The geopotential at the interfaces of the sigma layers is calculated integrating a finite difference approximation to the hydrostatic equation. This procedure is subject to an unavoidable error arising due to the finite differencing. However, this error is not peculiar to the sigma system. It occurs in the pressure system as well. For this reason we shall ignore it for a moment. An additional error in the sigma system may occur as a consequence of the assumption that the geopotential vary linearily with ς within the layers. This assumption is inherent in the hydrostatically consistent formula (19). Namely, when deriving this formula we have used the linear interpolation to define the geopotential at the pressure level corresponding to ς^*. However, the deviation of the geopotential from the linear profile may be large and, therefore, may affect considerably the accuracy of the pressure gradient force. This situation is visualized in Figure 8, the dashed lines representing the "true" profiles.

The situation is essentially the same with the formula (11) corresponding to the non-staggered distribution. Namely, in this case we have also assumed that the geopotential vary linearily with ς in between the sigma level at which the geopotential is defined, and the pressure level at which the pressure gradient force is calculated.

The error which we have discussed so far cannot be eliminated unless the geopotential is a linear function of ς. Obviously, only in this case the linear interpolation will be error-free. Therefore, it appears desirable to minimize the vertical variation

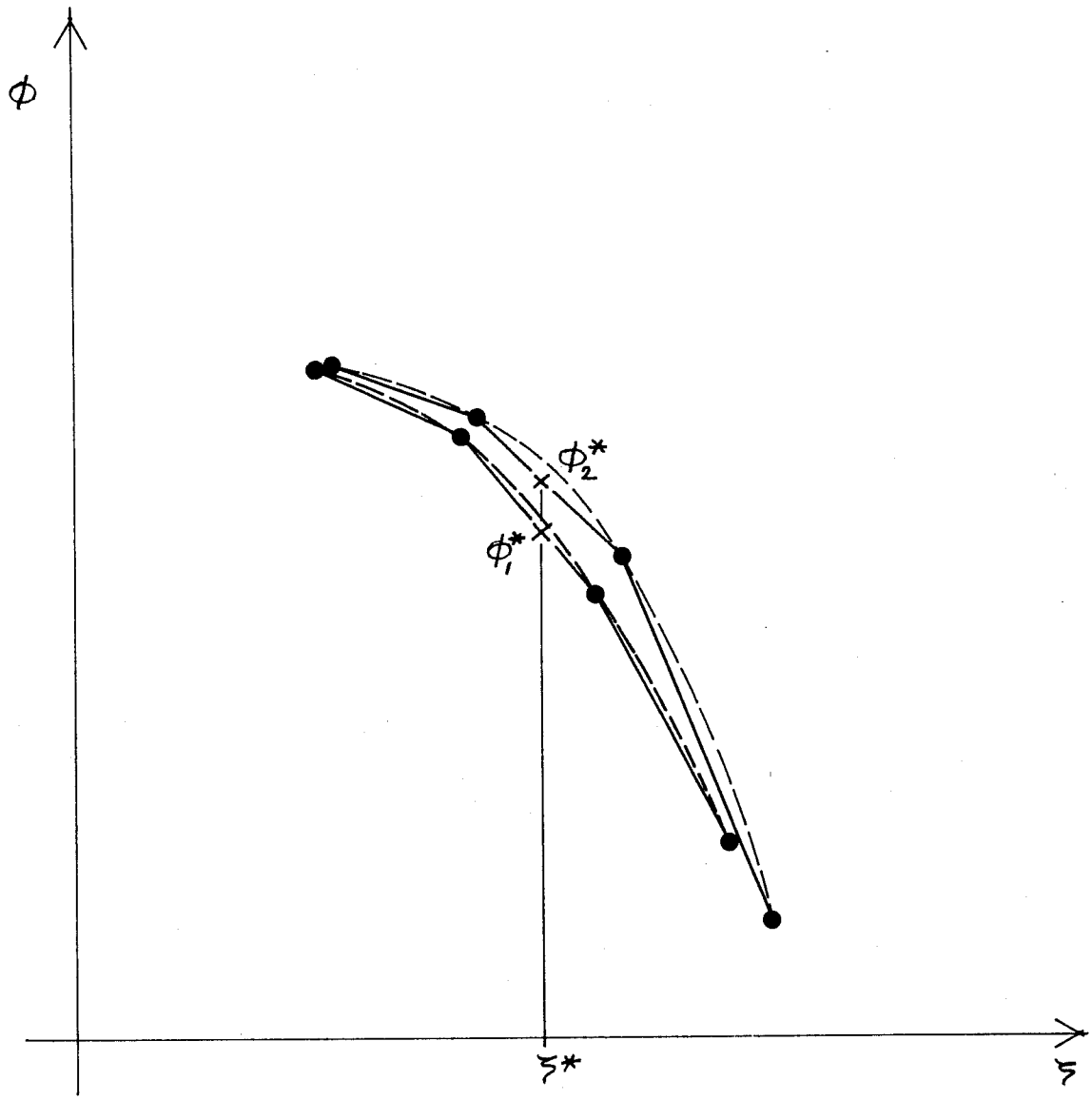

Figure 8. A schematic representation of the geopotential profiles at two adjacent grid points in the sigma system.

of the derivative of geopotential with respect to ζ. Apparently, the error introduced when calculating the geopotential at the interfaces would be minimized in this way as well. We can try to do this by a suitable choice of the function ζ. Namely, consider the hydrostatic equation of the form

$$\frac{\partial \phi}{\partial p} = -\frac{RT}{p} \quad . \tag{20}$$

Introducing the function ζ the equation (20) can be rewritten in the form

$$\frac{\partial \phi}{\partial \zeta} = -\frac{RT}{p \frac{d\zeta}{dp}} \tag{21}$$

If

$$\frac{\partial^2 \phi}{\partial \zeta^2} \equiv 0 , \tag{22}$$

there can be no variation of the derivative of geopotential with ζ. This will be the case if

$$p \frac{d\zeta}{dp} = CT \tag{23}$$

and C is a constant. Solving the equation (23) we can find an optimum form of the function ζ for any given temperature profile. However, we may be interested to minimize the error for a set of temperature profiles, rather than for a particular one. In this case instead of (23) we may require that, e.g., the vertical integral of the second derivative of geopotential with respect to ζ take on a minimum value. In this way, we may hope that the error will be minimized "in the mean". An example demonstrating how this procedure can be used will be given in the next section.

5. The choice of the function ζ – an example

Let us assume that the function ζ has the form

$$\zeta = x^{1+m} \tag{24}$$

where

$$x = \ln p \tag{25}$$

The hydrostatic equation then has the form

$$\frac{\partial \phi}{\partial \zeta} = -\frac{R}{1+m}\,\frac{T}{x^m} \tag{26}$$

To minimize the interpolation error the parameter m should be chosen in such a way that the second derivative of geopotential with respect to ζ is minimized. It can be verified in a straightforward manner that

$$\frac{\partial^2 \phi}{\partial \zeta^2} = -R\; e^{-2\ln(1+m) - (2m+1)\ln x}\left[x\frac{\partial T}{\partial x} - mT\right] \tag{27}$$

and

$$\frac{\partial}{\partial m}\frac{\partial^2 \phi}{\partial \zeta^2} = -R\, e^{-2\ln(1+m) - (2m+1)\ln x}\left[\left(\frac{2}{1+m} + 2\ln x - \frac{1}{m}\right)mT - \left(\frac{2}{1+m} + 2\ln x\right)x\frac{\partial T}{\partial x}\right]. \tag{28}$$

We may now require the expression (28) to vanish "in the mean", i.e.,

$$\int_{x_t}^{x_s} \frac{\partial}{\partial m}\frac{\partial^2 \phi}{\partial \zeta^2}\, dx = 0\,. \tag{29}$$

Here x_t and x_s are the values of x at the top and at the bottom of the model's atmosphere. The equation (29) is rather difficult to solve for m. If we assume that the top of the model's atmosphere is located at, e.g., 200 mb, using approximate methods, we find that m takes on a value in between 1 and 2. This is a very crude

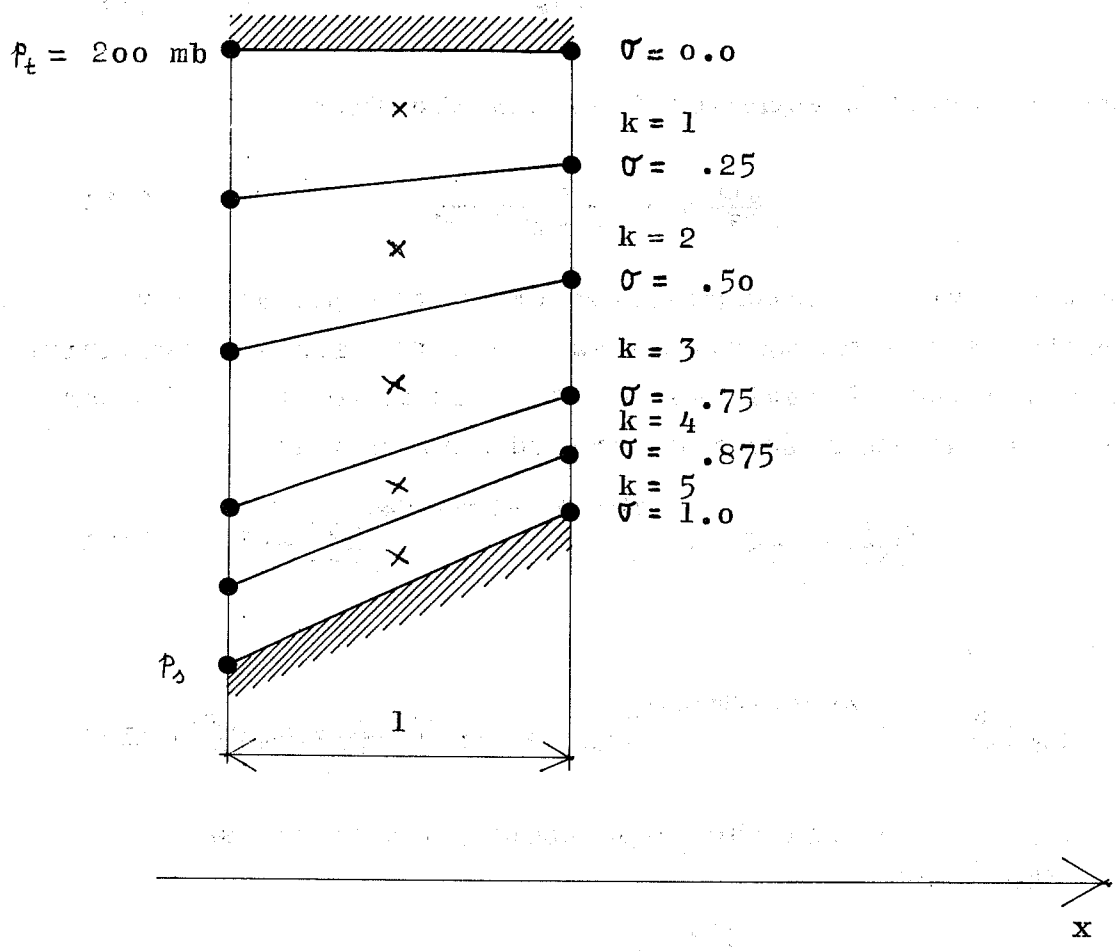

Figure 9. Schematic representation of the vertical discretization used in the numerical test.

m		k = 1	k = 2	k = 3	k = 4	k = 5
0.0	term I	4577.6	11177	14464	16221	17142
	term II	− 4423.7	− 11120	− 14439	− 16222	− 17144
	error	153.95	56.852	25.066	− 0.5508	− 2.6641
0.2	term I	4577.6	11177	14464	16221	17142
	term II	− 4450.2	− 11125	− 14441	− 16221	− 17144
	error	127.43	51.590	23.250	0.0391	− 2.0391
0.4	term I	4577.6	11177	14464	16221	17142
	term II	− 4477.4	− 11131	− 14443	− 16221	− 17144
	error	100.25	45.477	21.086	0.1484	− 1.8711
0.6	term I	4577.6	11177	14464	16221	17142
	term II	− 4504.5	− 11138	− 14445	− 16222	− 17143
	error	73.141	39.383	19.504	− 0.5234	− 1.3359
0.8	term I	4577.6	11177	14464	16221	17142
	term II	− 4531.6	− 11144	− 14448	− 16221	− 17144
	error	46.012	33.141	16.688	0.1172	− 2.2969
1.0	term I	4577.6	11177	14464	16221	17142
	term II	− 4559.1	− 11150	− 14450	− 16222	− 17144
	error	18.543	26.773	14.633	− 0.4258	− 1.9531
1.2	term I	4577.6	11177	14464	16221	17142
	term II	− 4586.4	− 11156	− 14453	− 16222	− 17144
	error	− 8.7891	20.488	11.859	− 0.5859	− 2.5781
1.4	term I	4577.6	11177	14464	16221	17142
	term II	− 4614.2	− 11163	− 14455	− 16222	− 17144
	error	− 36.559	13.828	9.4219	− 1.0859	− 2.2930
1.6	term I	4577.6	11177	14464	16221	17142
	term II	− 4641.8	− 11170	− 14458	− 16223	− 17144
	error	− 64.180	7.2659	6.9141	− 2.0859	− 2.2188
1.8	term I	4577.6	11177	14464	16221	17142
	term II	− 4669.5	− 11177	− 14461	− 16223	− 17145
	error	− 91.863	0.3672	3.7109	− 1.9258	− 3.5938
2.0	term I	4577.6	11177	14464	16221	17142
	term II	− 4697.4	− 11183	− 14464	− 16224	− 17146
	error	− 119.82	− 6.5391	0.9023	− 2.9336	− 3.8047

Table 1. The first and the second term of the pressure gradient force approximation as well as their sum as a function of parameter m. All values are given in m^2/sec^2.

estimate, however. In a similar way it can be shown that the optimum value of m in the sense of the formula (29) is decreasing with increasing the height of the top of the model's atmosphere. It should also be kept in mind that the formula (29) disregards the inversions.

As a compromise between the requirements for minimization of the interpolation error and for computational economy, if the top of the model's atmosphere is located at 2oo mb, we can choose the value $m=1$. The finite difference hydrostatic equation then has the form

$$\delta_z \phi_k = -R \frac{T_k}{2 \ln p_k} \cdot \qquad (3o)$$

We can define the logarithm of pressure within the layer e.g. by

$$\ln p_k = \frac{1}{2}(\ln p_{k-1/2} + \ln p_{k+1/2}) \cdot \qquad (31)$$

This form of the hydrostatic equation is used in the HIBU (Hydrometeorological Institutes and Belgrade University) model (Janjić 1977, 1979; Mesinger 1977) and in the family of models developed from it (e.g. Buzzi et al. 1979; Mesinger 1979).

To test the performance of the proposed method, a numerical test almost identical to that of Phillips (1974) was performed. Namely, we examined the artificial value of $-\nabla_p \phi$ introduced by the sigma system when the geopotential was only a function of pressure, i.e. in the atmosphere with zero analytic pressure gradient force. The geopotential profile was assumed to be of the form

$$\phi = 1o54.5 + 8o397.3\, z - 7659.o\, z^2 + 111o.o\, z^3 \qquad (32)$$

where

$$z = -x + 11.51292546 \quad . \tag{33}$$

Here the SI system of units is used. As in the Phillips' (1974) experiment, we considered two columns located along, say, x-axis at a unit distance from each other. The surface pressure at these two points was assumed to be 800 mb and 1000 mb respectively. According to (32), the corresponding values of the surface geopotential were 18625.727 m^2/sec^2 and 1054.5 m^2/sec^2. The sigma coordinate was defined by

$$\sigma = \frac{p - p_t}{\pi} \tag{34}$$

where

$$\pi = p_s - p_t \tag{35}$$

and p_s and p_t were the values of pressure at the earth's surface and at the top of the model's atmosphere which was situated at 200 mb. The interfaces of the layers were located at the sigma surfaces 0., .25, .50, .75, .875 and 1. This situation is shown schematically in Figure 9. The hydrostatically consistent formula (19) was applied at the points marked by crosses in the figure. As in the Phillips' test, the geopotential at the interfaces, located at the points denoted by heavy dots in the figure, was prescribed using the analytic expression (32). Thus, only the linear interpolation error was left.

The values of the first and the second term on the right hand side of formula (19), as well as the values of their sums, for different values of the parameter m are summarized in Table 1. These sums

should ideally cancel. Note that due to very steep slope of the sigma surfaces we may have a situation similar to that of Figure 7 within the two lowest layers. However, as it can be seen from the table, in this case the error is generally of the order of the round-off error and shows erratic behaviour with variation of m. On the other hand, at higher levels there is a reasonable agreement between the experimental results and the theoretical considerations. Namely, the results indicate that the proposed method for minimizing the pressure gradient force error acts in the right direction.

6. False vertical staggering of the pressure gradient and Coriolis force

As we have noticed, the formula (18) can be considered as the definition of the height at which the pressure gradient force, and therefore the corresponding velocity component, is being calculated. In certain cases, however, this definition may imply false vertical staggering of the pressure gradient and Coriolis force if the formula (19) is applied in the most straightforward way. Namely, the two velocity components may be defined at different pressure levels. In case of steep topography, the variation of velocity in between the two pressure levels may be considerable. Thus, noticeable errors may be made when calculating the Coriolis term. As a consequence, the meaning of the geostrophic balance in the model's atmosphere in the vicinity of the mountains may be considerably altered.

The problem which we are discussing is to a certain extent related to the choice of the distribution of dependent variables in the horizontal. Three possibilities denoted by B, E and C are shown in

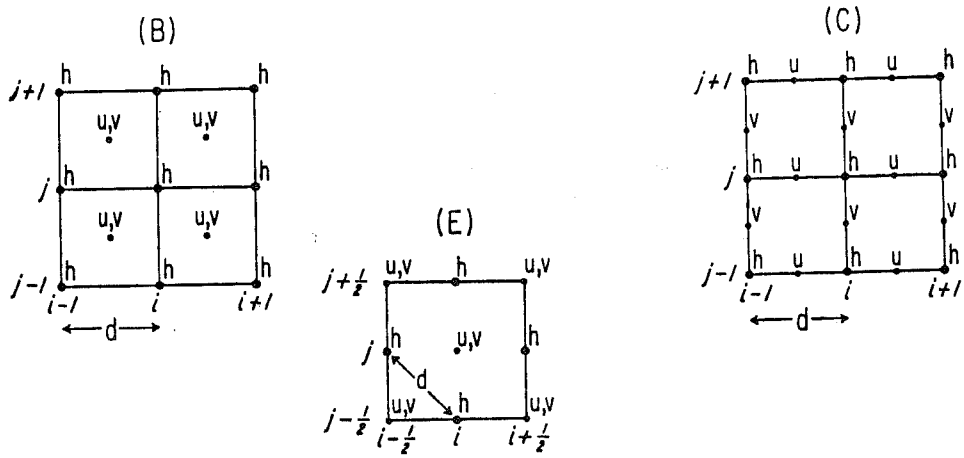

Figure 10. Grids B, E and C.

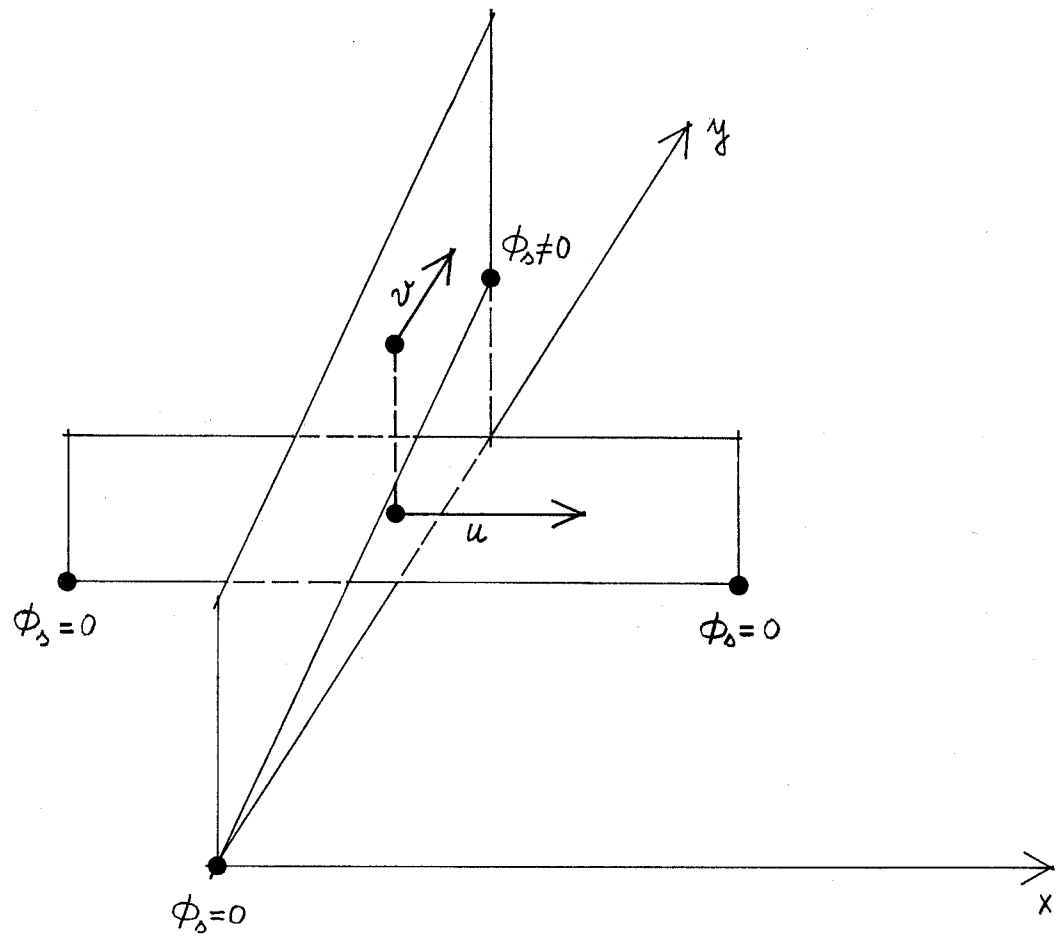

Figure 11. False vertical staggering of velocity components on the E grid.

Figure 10. In Figure 11 the E grid is used as an example to visualize the false vertical staggering of the velocity components. The symbol ϕ_s is used in the figure to denote the geopotential at the ground surface at the grid points marked by heavy dots. The two intersecting rectangles represent schematically the segments of the lowest sigma layer in between the grid points, as viewed in the direction of the x and y-axis respectively. A similar example can be constructed for the C grid.

The situation is rather different in case of the E grid. Namely, assuming that the y-axis is oriented northward, the x-component of the pressure gradient force is calculated as an arithmetic mean of the contributions half a grid length south and half a grid length north of the velocity point. The southern contribution is calculated at the level

$$\zeta_S^* = \overline{\overline{\zeta}^{\sigma}}^{x} \tag{36}$$

and the northern one at the level

$$\zeta_N^* = \overline{\overline{\zeta}^{\sigma}}^{x} \quad . \tag{37}$$

The level at which the mean value is located is not explicitly specified. However, assuming that both the x-component of the pressure gradient force and ζ vary linearily with y in between the points at which the southern and the northern contributions are calculated, this level is defined by

$$\zeta_x^* = \tfrac{1}{2}\left(\overline{\zeta_S^{\sigma}}^{x} + \overline{\zeta_N^{\sigma}}^{x}\right) = \overline{\overline{\zeta^{\sigma}}^{x}}^{y} \quad . \tag{38}$$

Here, the averaging operator with respect to y is defined analogously to that applied in the direction of the x-axis. Similar considerations for

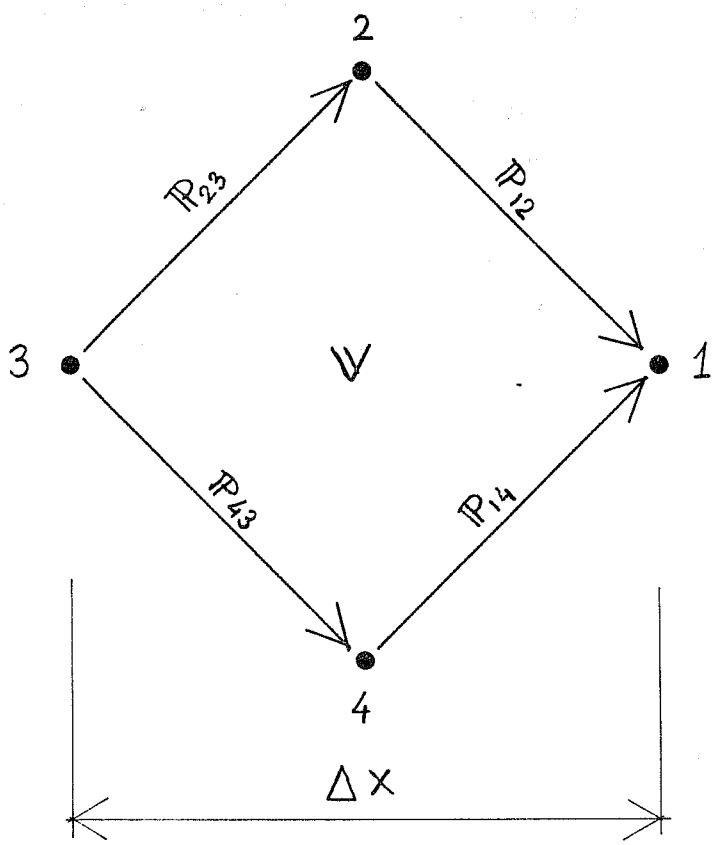

Figure 12. Stencil used to define an approximation to the pressure gradient force on the E grid.

the y-component show that the level at which this component is calculated is defined by

$$\zeta_y^* = \overline{\overline{\zeta}^{\sigma}}^{yx} \quad . \tag{39}$$

Having in mind the definitions of the averaging operators, we find that

$$\zeta_x^* = \zeta_y^* \quad , \tag{40}$$

i.e. the both components are defined at the same level.

To avoid this problem on the E grid Janjić (1977) proposed to apply an averaging technique analogous to that applied on the B grid. Namely, using the notation introduced in Figure 12, the x-component of the pressure gradient force can be calculated according to the formula

$$-\delta_x \overline{\Phi}^{\sigma} + \tilde{\pi} \cdot \mathbb{C} = -\frac{1}{2\Delta x} \tilde{\pi} \cdot [\mathbb{P}_{23} + \mathbb{P}_{12} + \mathbb{P}_{43} + \mathbb{P}_{14}] \tag{41}$$

where

$$\begin{aligned}
|\mathbb{P}_{23}| &= \overline{\Phi}_2^{\sigma} - \overline{\Phi}_3^{\sigma} - \tfrac{1}{2}(\delta_\zeta \Phi_2 + \delta_\zeta \Phi_3)(\overline{\zeta}_2^{\sigma} - \overline{\zeta}_3^{\sigma}) \\
|\mathbb{P}_{12}| &= \overline{\Phi}_1^{\sigma} - \overline{\Phi}_2^{\sigma} - \tfrac{1}{2}(\delta_\zeta \Phi_1 + \delta_\zeta \Phi_2)(\overline{\zeta}_1^{\sigma} - \overline{\zeta}_2^{\sigma}) \\
|\mathbb{P}_{43}| &= \overline{\Phi}_4^{\sigma} - \overline{\Phi}_3^{\sigma} - \tfrac{1}{2}(\delta_\zeta \Phi_4 + \delta_\zeta \Phi_3)(\overline{\zeta}_4^{\sigma} - \overline{\zeta}_3^{\sigma}) \\
|\mathbb{P}_{14}| &= \overline{\Phi}_1^{\sigma} - \overline{\Phi}_4^{\sigma} - \tfrac{1}{2}(\delta_\zeta \Phi_1 + \delta_\zeta \Phi_4)(\overline{\zeta}_1^{\sigma} - \overline{\zeta}_4^{\sigma}) \quad .
\end{aligned} \tag{42}$$

For brevity, the symbol $\mathbb{C}$ has been introduced to denote the finite difference approximation to the second term

on the right hand side of (8). It can be verified that provided the y-component is calculated analogously, we shall have the situation similar to that on the B grid. This averaging technique is applied in the HIBU model and in the family of models derived from it.

In contrast to the grids B and E, it is rather difficult to see what can be done to avoid the false vertical staggering in case of the C grid.

7. Pressure gradient force and energy conservation

For a number of the pressure gradient force schemes an associated procedure for calculation of the omega-alpha term of the thermodynamic equation ensuring consistency in transformation between the kinetic and potential energy has also been developed. Experience has shown that it is desirable to preserve this consistency even in numerical models designed for short-range simulations. Otherwise the numerical instability may be encountered after less than a day of simulation time in the presence of steep topography.

As we have seen, the procedure described in Section 4 may lead to rather unusual finite difference forms of the hydrostatic equation. For this reason, in this section we shall derive a general scheme for the omega-alpha term of the thermodynamic equation corresponding to the general form of the pressure gradient force approximation in case of the staggered distribution of variables in the vertical. For the sake of completeness, however, we shall start with the continuous equations.

The kinetic energy generation due to the pressure gradient force, per unit mass, is given by

$$-\mathbf{v}\cdot\nabla_p\phi = -\mathbf{v}\cdot\nabla_\sigma\phi + \mathbf{v}\cdot\frac{\partial\phi}{\partial\varsigma}\nabla_\sigma\varsigma \quad . \tag{43}$$

Multiplying the expression (43) by a mass element

$$dm = -\frac{1}{g}\pi\, dA\, d\sigma \tag{44}$$

we obtain

$$-\mathbf{v}\cdot\nabla_p\phi\, dm = -\frac{1}{g}\left[-\pi\mathbf{v}\cdot\nabla_\sigma\phi + \pi\mathbf{v}\cdot\frac{\partial\phi}{\partial\varsigma}\nabla_\sigma\varsigma\right] dA\, d\sigma \tag{45}$$

Here dA is an area element and the other symbols used have either their usual meaning, or they have already been defined. Taking into account the identities

$$\pi\mathbf{v}\cdot\nabla_\sigma\phi = \nabla_\sigma\cdot(\pi\mathbf{v}\phi) - \phi\,\nabla_\sigma\cdot(\pi\mathbf{v}), \tag{46}$$

$$\frac{\partial\phi}{\partial\varsigma}\nabla_\sigma\varsigma = \frac{1}{\pi}\frac{\partial\phi}{\partial\sigma}\nabla_\sigma p \ , \tag{47}$$

as well as the continuity equation

$$\nabla_\sigma\cdot(\pi\mathbf{v}) = -\frac{\partial\pi}{\partial t} - \frac{\partial}{\partial\sigma}(\pi\dot{\sigma}) \ , \tag{48}$$

the equation (45)may be rewritten in the form

$$-\mathbf{v}\cdot\nabla_p\phi\, dm = -\frac{1}{g}\left[-\nabla_\sigma\cdot(\pi\mathbf{v}\phi) - \phi\frac{\partial\pi}{\partial t} - \phi\frac{\partial}{\partial\sigma}(\pi\dot{\sigma}) - \mathbf{v}\cdot\left(\frac{\partial\phi}{\partial\sigma}\nabla_\sigma p\right)\right] dA\, d\sigma. \tag{49}$$

However, since

$$\phi\frac{\partial\pi}{\partial t} + \phi\frac{\partial}{\partial\sigma}(\pi\dot{\sigma}) = \frac{\partial}{\partial\sigma}\left(\phi\sigma\frac{\partial\pi}{\partial t} + \phi\pi\dot{\sigma}\right) - \sigma\frac{\partial\phi}{\partial\sigma}\frac{\partial\pi}{\partial t} - \pi\dot{\sigma}\frac{\partial\phi}{\partial\sigma} \ , \tag{50}$$

the equation (49) takes the form

$$-\nabla\cdot\nabla_p\phi\,dm = -\frac{1}{g}\Big[-\nabla_\sigma\cdot(\pi\nabla\phi)-\frac{\partial}{\partial\sigma}\Big(\phi\sigma\frac{\partial\pi}{\partial t}+\phi\pi\dot\sigma\Big)$$

$$+\sigma\frac{\partial\phi}{\partial\sigma}\frac{\partial\pi}{\partial t}+\pi\dot\sigma\frac{\partial\phi}{\partial\sigma}+\nabla\cdot\Big(\frac{\partial\phi}{\partial\sigma}\nabla_\sigma p\Big)\Big]dA\,d\sigma\ . \tag{51}$$

Taking into account the hydrostatic equation

$$\frac{\partial p}{\partial\sigma} = -\pi\alpha \tag{52}$$

instead of (51) we may write

$$-\nabla\cdot\nabla_p\phi\,dm = -\frac{1}{g}\Big[-\nabla_\sigma\cdot(\pi\nabla\phi)-\frac{\partial}{\partial\sigma}\Big(\phi\sigma\frac{\partial\pi}{\partial t}+\phi\pi\dot\sigma\Big)$$

$$-\pi\alpha\dot\sigma\frac{\partial p}{\partial\sigma}-\pi\alpha\nabla\cdot\nabla_\sigma p\Big]\,dA\,d\sigma\ , \tag{53}$$

and finally,

$$-\nabla\cdot\nabla_p\phi\,dm = -\frac{1}{g}\Big[-\nabla_\sigma\cdot(\pi\nabla\phi)-\frac{\partial}{\partial\sigma}(\phi\pi\dot\sigma)-\frac{\partial}{\partial\sigma}\Big(\phi\sigma\frac{\partial\pi}{\partial t}\Big)-\pi\omega\alpha\Big]dA\,d\sigma \tag{54}$$

where

$$\omega = \frac{dp}{dt} = \frac{\partial p}{\partial t}+\nabla\cdot\nabla_\sigma p+\dot\sigma\frac{\partial p}{\partial\sigma}\ . \tag{55}$$

Integrating the equation (54) over a closed domain, the contribution of the first term in square brackets vanishes. Provided $\dot\sigma=0$ at the top and at the bottom of the model's atmosphere, the same is true for the second term when the integration is performed with respect to sigma. The contribution of the last term in the square brackets cancels in the total energy equation with the contribution of the omega-alpha term of the thermodynamic equation which enters the total energy equation with the opposite sign.

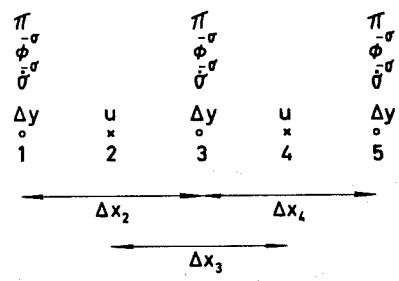

Figure 13. Stencil used to derive an energy conserving scheme for the omega-alpha term of the thermodynamic equation.

Let us now proceed with the discrete equations. For convenience we shall treat the two terms of the pressure gradient force separately. Let us start with the first one as defined by the formulae (19) and (41). Namely, consider the stencil of grid points shown in Figure 13. It does not imply any particular choice of the distribution of variables over grid points since it represents a subset of most of commonly used grids. Note that we do not require the grid distances to be constant. Let the symbol π_* denote the value of π at velocity points, and let a mass element be defined by

$$\Delta m = -\frac{1}{g}\pi_* \Delta x \Delta y \Delta\sigma . \tag{56}$$

Using the notation introduced in Figure 13 we may write

$$-\tfrac{1}{2}\left[(\Delta m u \delta_x \overline{\Phi}^{\sigma})_4 + (\Delta m u \delta_x \overline{\Phi}^{\sigma})_2\right] = \frac{1}{g}\left\{\tfrac{1}{2}(\pi_* u)_4 \frac{\overline{\Phi_5}^{\sigma} - \overline{\Phi_3}^{\sigma}}{\Delta x_4}\Delta x_4 \Delta y_4 + \tfrac{1}{2}(\pi_* u)_2 \frac{\overline{\Phi_2}^{\sigma} - \overline{\Phi_1}^{\sigma}}{\Delta x_2}\Delta x_2 \Delta y_2\right\}\Delta\sigma . \tag{57}$$

The right hand side of this identity can be written in the form

$$\begin{aligned} -\tfrac{1}{2}\left[(\Delta m u \delta_x \overline{\Phi}^{\sigma})_4 + (\Delta m u \delta_x \overline{\Phi}^{\sigma})_2\right] = \frac{1}{g}\Big\{ & \tfrac{1}{2}\overline{\Phi_3}^{\sigma}\left[(\pi_* u_4)\Delta y_4 - (\pi_* u_2)\Delta y_2\right] - \tfrac{1}{2}\overline{\Phi_5}^{\sigma}(\pi_* u)_4 \Delta y_4 + \tfrac{1}{2}\overline{\Phi_1}^{\sigma}(\pi_* u)_2 \Delta y_2 \\ & + \tfrac{1}{2}\overline{\Phi_3}^{\sigma}(\pi_* u)_4 \Delta y_4 - \tfrac{1}{2}\overline{\Phi_3}^{\sigma}(\pi_* u)_4 \Delta y_4 + \tfrac{1}{2}\overline{\Phi_3}^{\sigma}(\pi_* u)_2 \Delta y_2 - \tfrac{1}{2}\overline{\Phi_3}^{\sigma}(\pi_* u)_2 \Delta y_2 \Big\}\Delta\sigma . \end{aligned} \tag{58}$$

After rearrangement, instead of (58) we may write

$$\begin{aligned} -\tfrac{1}{2}\left[(\Delta m u \delta_x \overline{\Phi}^{\sigma})_4 + (\Delta m u \delta_x \overline{\Phi}^{\sigma})_2\right] = \frac{1}{g}\Big\{ & \overline{\Phi_3}^{\sigma}\frac{(\pi_* u)_4 \Delta y_4 - (\pi_* u)_2 \Delta y_2}{\Delta x_3 \Delta y_3} \\ & - \frac{\tfrac{1}{2}(\overline{\Phi_5}^{\sigma} + \overline{\Phi_3}^{\sigma})(\pi_* u)_4 \Delta y_4 - \tfrac{1}{2}(\overline{\Phi_3}^{\sigma} + \overline{\Phi_1}^{\sigma})(\pi_* u)_2 \Delta y_2}{\Delta x_3 \Delta y_3}\Big\}\Delta x_3 \Delta y_3 \Delta\sigma \end{aligned} \tag{59}$$

or, in a more compact form,

$$\overline{-u \delta_x \overline{\Phi}^{\sigma} \Delta m}^{x} = \frac{1}{g}\left\{\overline{\Phi}^{\sigma_1}_{\Delta y}\delta_x(\pi_* u \Delta y) - \frac{1}{\Delta y}\delta_x(\overline{\Phi}^{\sigma\,x}\pi_* u \Delta y)\right\}\Delta x \Delta y \Delta\sigma . \tag{60}$$

Obviously, in the direction of the y-axis we shall have a similar situation. Namely, starting from an identity analogous to (57) we arrive to the expression

$$\overline{-v\delta_y\overline{\Phi}^{\sigma}\Delta m}^{y}=\frac{1}{g}\left\{\overline{\Phi}^{\sigma}\frac{1}{\Delta x}\delta_y(\pi_* v\Delta x)-\frac{1}{\Delta x}\delta_y(\overline{\Phi}^{\sigma y}\pi_* u\Delta x)\right\}\Delta x\Delta y\Delta\sigma\ . \qquad (61)$$

Summing the expressions (6o) and (61) we obtain

$$\overline{-u\delta_x\overline{\Phi}^{\sigma}\Delta m}^{x}-\overline{v\delta_y\overline{\Phi}^{\sigma}\Delta m}^{y}=\frac{1}{g}\left\{\overline{\Phi}^{\sigma}\nabla_\sigma\cdot(\pi_* v)-\nabla_\sigma\cdot(\widetilde{\overline{\Phi}^{\sigma}}\pi_* v)\right\}\Delta x\Delta y\Delta\sigma. \qquad (62)$$

Here ∇_σ is the simplest finite difference approximation to the ∇ operator applied at a constant sigma surface and the averaging operator $\sim$ denotes the two-point mean calculated in the direction of velocity components. Summing up the expressions (62) over a closed domain and all values of the vertical index, we obtain

$$\sum-v\cdot\nabla_\sigma\overline{\Phi}^{\sigma}\Delta m=\frac{1}{g}\sum\overline{\Phi}^{\sigma}\nabla_\sigma\cdot(\pi_* v)\Delta x\Delta y\Delta\sigma-\frac{1}{g}\sum\nabla_\sigma\cdot(\widetilde{\overline{\Phi}^{\sigma}}\pi_* v)\Delta x\Delta y\Delta\sigma\ . \qquad (63)$$

On the left hand side of this expression we recognize the contribution of the first term of the pressure gradient force to the overall kinetic energy generation. Since the summation is performed over a closed domain, the second term on the right hand side of (63) vanishes. Thus, this feature of the continuous atmosphere is reproduced without any additional effort. On the other hand, taking into account the finite difference approximation to the continuity equation we may write

$$\overline{\Phi}^{\sigma}\nabla_\sigma\cdot(\pi_* v)=-\overline{\Phi}^{\sigma}\frac{\partial\pi}{\partial t}-\overline{\Phi}^{\sigma}\delta_\sigma(\pi\dot{\sigma})\ , \qquad (64)$$

and finally,

$$\overline{\Phi}^{\sigma}\nabla_\sigma\cdot(\pi_* v)=-\delta_\sigma(\Phi\pi\dot{\sigma})-\delta_\sigma(\Phi\sigma\frac{\partial\pi}{\partial t})+\overline{\sigma}^{\sigma}\delta_\sigma\Phi\frac{\partial\pi}{\partial t}+\pi\overline{\dot{\sigma}}^{\sigma}\delta_\sigma\Phi\ . \qquad (65)$$

Substituting (65) into (63) we obtain

$$\Sigma -\nabla\cdot\nabla_\sigma \overline{\phi}^{\sigma}\Delta m=-\frac{1}{g}\Sigma\delta_\sigma(\phi\pi\dot\sigma)\Delta x\Delta y\Delta\sigma-\frac{1}{g}\Sigma\delta_\sigma(\phi\sigma\frac{\partial\pi}{\partial t})\Delta x\Delta y\Delta\sigma$$

$$+\frac{1}{g}\Sigma\overline{\sigma}^{\sigma}\delta_\sigma\phi\frac{\partial\pi}{\partial t}\Delta x\Delta y\Delta\sigma+\frac{1}{g}\Sigma\pi\overline{\dot\sigma}^{\sigma}\delta_\sigma\phi\Delta x\Delta y\Delta\sigma\ . \tag{66}$$

As in the continuous case, provided $\dot\sigma=0$ at the top and at the bottom of the model's atmosphere, the first term on the right hand side of (66) vanishes. When the grid size tends to zero, the last two terms tend to

$$\frac{1}{g}\Sigma\overline{\sigma}^{\sigma}\delta_\sigma\phi\frac{\partial\pi}{\partial t}\Delta x\Delta y\Delta\sigma\longrightarrow\int\alpha\frac{\partial p}{\partial t}dm$$

$$\frac{1}{g}\Sigma\pi\overline{\dot\sigma}^{\sigma}\delta_\sigma\phi\Delta x\Delta y\Delta\sigma\longrightarrow\int\alpha\dot\sigma\frac{\partial p}{\partial\sigma}dm\ . \tag{67}$$

Therefore, if within the omega-alpha term of the thermodynamic equation we use the approximations

$$\alpha\frac{\partial p}{\partial t}\Rightarrow-\overline{\sigma}^{\sigma}\frac{1}{\pi}\frac{\partial\pi}{\partial t}\delta_\sigma\phi$$

$$\alpha\dot\sigma\frac{\partial p}{\partial\sigma}\Rightarrow-\overline{\dot\sigma}^{\sigma}\delta_\sigma\phi\ , \tag{68}$$

the overall contribution of these terms to the total energy change rate will compensate exactly the contributions of the last two terms in the equation (66), as in the case of continuous equations. It should be noted that the approximations (68) do not imply any particular choice of the hydrostatic equation. Only the values of geopotential at the interfaces of the layers and the corresponding values of the sigma coordinate should be known.

Let us now consider the second term of the pressure gradient force, which we shall denote by as before. Its overall contribution to the kinetic energy generation is given by

$$\sum \mathbf{C}\cdot\mathbf{V}\Delta m = \sum \pi_* \mathbf{V}\cdot\mathbf{C}\,\Delta x\Delta y\Delta\sigma \,. \qquad (69)$$

Here the summation sign has the same meaning as before. When the grid size tends to zero, as we can infere from (47), the expression (69) tends to

$$\sum \pi_* \mathbf{V}\cdot\mathbf{C}\,\Delta x\Delta y\Delta\sigma \longrightarrow \int \alpha\,\mathbf{V}\cdot\nabla_\sigma p\,dm \,. \qquad (70)$$

This gives us an idea how to design the finite difference approximation to the remaining part of the omega-alpha term corresponding to the horizontal advection of pressure along the sigma surface. Let us consider the C grid first. If we use the approximation

$$\alpha\mathbf{V}\cdot\nabla_\sigma p \Rightarrow \frac{1}{\pi}\left(\pi_* u\,\overline{\delta_\zeta \phi}^{\,x}\delta_x \overline{\zeta}^{\sigma}{}^{x} + \pi_* v\,\overline{\delta_\zeta \phi}^{\,y}\delta_y \overline{\zeta}^{\sigma}{}^{y}\right) \qquad (71)$$

the overall contribution of this term to the total energy change rate will compensate exactly the contribution of the expression (67) as in the case of continuous equations. Namely, multiplying (71) by

$$\Delta m_h = -\frac{1}{g}\pi\,\Delta x\Delta y\,\Delta\sigma \qquad (72)$$

and summing up, we obtain an expression identical to (69) which enters the total energy equation with the opposite sign.

The approximation (71) could be used on the E grid as well. However, since it would imply the separate cancellation on the two C subgrids of this grid, it might be advantageous to use the approximation

of the form

$$\propto \mathbf{v}\cdot\nabla_\sigma p \Rightarrow \frac{1}{\pi}\,\overline{(\pi_* \mathbf{v}\cdot\mathbf{c})}^{xy} \,. \qquad (73)$$

Here the averaging operator denotes a mean value at a mass field point calculated from the values at four nearest velocity points. The approximation (73) is used in the HIBU model and in the family of models derived from it.

References

Arakawa, A., 1972: Design of the UCLA general circulation model. Technical Report No. 7, Dept. of Meteorology, University of California, 116 pp.

Arakawa, A., and V.R. Lamb, 1977: Computational design of the basic dynamical processes of the UCLA general circulation model. Methods in Comp. Physics 17, 173-265.

Arakawa, A., and Y. Mintz, 1974: The UCLA atmospheric general circulation model, Notes distributed at the Workshop 25 March-4 April 1974, Dept. of Meteorology, Univ. of California, Los Angeles.

Brown, J.A. Jr., 1974: On vertical differencing in the sigma system. Office Note No. 92, National Meteorological Center, NOAA/NWS, U.S. Department of Commerce, 12 pp.

Buzzi, A., Malguzzi, P. and Tibaldi, S., 1979: Orographically induced cyclogenesis: Analysis of numerical experiments. Paper presented to the Siegsdorf Euromech. Conference, 2-3 April 1979.

Corby, G.A., Gilchrist, A. and Newson, R.L., 1972: A general circulation model of the atmosphere suitable for long period integrations. Q.J. Roy. Met. Soc. 98, 809-832.

Gary, J.M., 1975: Estimate of truncation error in transformed coordinate, primative equation atmospheric models. J. Atmos. Sci., 30, 223-233.

Gilchrist, A., 1975: The Meteorological Office general circulation model. Seminars on Scientific Foundation of Medium Range Weather Forecasts, Part II, 594-661. European Centre for Medium Range Weather Forecasts, Reading, England.

Janjić, Z.I., 1977: Pressure gradient force and advection scheme used for forecasting with steep and small scale topography. Beitr. Phys. Atmosph., 50, 186-199.

Janjić, Z.I. 1979: Forward-backward scheme modified to prevent two-grid interval noise and its application in sigma coordinate models. To be published in Beitr. Phys. Atmosph., 52.

Kasahara, A., 1974: Various vertical coordinate systems used for numerical weather prediction. Mon. Wea. Rev., 102, 509-522.

Kasahara, A., 1977a: Computational aspects of numerical models for weather prediction and climate simulation. Methods in Comp. Phys., 17, 1-66.

Kasahara, A., 1977b: The effects of mountains on synoptic-scale flows. Paper presented at the First Planning Meeting on the GARP Mountain sub-programme, Venice 24-28 October 1977.

Kurihara, Y., 1968: Note on finite difference expressions for the hydrostatic relation and pressure gradient force. Mon. Wea. Rev., 96, 654-656.

Mesinger, F., 1977: Forward-backward scheme and its use in a limited area model. Beitr. Phys. Atmosph., 50, 200-210.

Mesinger, F., 1979a: Finite difference schemes of a staggered grid enstrophy and energy conserving model. In preparation for publication.

Mesinger, F., 1979b: Dependence of vorticity analogue and the Rossby wave phase speed on the choice of horizontal grid. Bulletin T. LXIV de l'Académie serbe des sciences et des arts, Classe des sciences mathématiques et naturelles, Sciences mathématiques No. 10, 5-15.

Phillips, N.A., 1957: A coordinate system having some special advantages for numerical forecasting. J. Meteor., 14, 184-185.

Phillips, N.A., 1974: Application of Arakawa's energy conserving layer model to operational numerical weather prediction. Office Note No. 104, National Meteorological Center, NOAA/NWS, U.S. Department of Commerce, 40.

Rousseau, D., and H.L. Pham, 1971: Premiers resultats d'un modèle de prévision numérique a courte echeance sur l'Europe. La Meteorologie, 20, 1-12.

Smagorinsky, J., Strickler, R.F., Sangster, W.E., Manabe, S., Holloway, J.L., Hembree, G.D., 1967: Prediction experiments with a general circulation model. Proc. International Symposium on Dynamics of Large Scale Atmospheric Processes, Moscow, USSR, 23-30 June 1965, Izdatel'stvo "Nauka", Moscow, 70-134.

Sundqvist, H. 1975a: On truncation errors in sigma-system models. Atmosphere, 13, 81-95.

Sundqvist, H. 1975b: Initialization for models using sigma as the vertical coordinate. J. Appl. Met., 14, 153-158.

Tokioka, T., 1978: Some considerations on vertical differencing. J. Met. Soc. Japan, 56, 98-111.